DNA Polymerase β: Contributions of Template-Positioning and dNTP Triphosphate-Binding Residues to Catalysis and Fidelity[†]

Vadim S. Kraynov,[‡] Alexander K. Showalter,[§] Jia Liu,[‡] Xuejun Zhong,[§] and Ming-Daw Tsai*[,‡,§,||]

Departments of Biochemistry and Chemistry, The Ohio State University, Columbus, Ohio 43210

Received April 14, 2000; Revised Manuscript Received July 12, 2000

ABSTRACT: The specific catalytic roles of two groups of DNA polymerase β active site residues identified from crystal structures were investigated: residues possibly involved in DNA template positioning (Lys280, Asn294, and Glu295) and residues possibly involved in binding the triphosphate moiety of the incoming dNTP (Arg149, Ser180, Arg183, and Ser188). Eight site-specific mutants were constructed: K280A, N294A, N294Q, E295A, R149A, S180A, R183A, and S188A. Two-dimensional NMR analysis was employed to show that the global conformation of the mutants has not been perturbed significantly. Pre-steady-state kinetic analyses with single-nucleotide gapped DNA substrates were then performed to obtain the rate of catalysis at saturating dNTP (k_{pol}), the apparent dissociation constant for dNTP (K_d), catalytic efficiency k_{pol}/K_d, and fidelity. Of the three template-positioning residues, Asn294 and Glu295 (but not Lys280) contribute significantly to k_{pol}. Taken together with other data, the results suggest that these two residues help to stabilize the transition state during catalysis even though they interact with the DNA template backbone rather than directly with the incoming dNTP or the opposite base on the template. Furthermore, the fidelity increases by up to 19-fold for N294Q due to differential k_{pol} effects between correct and incorrect nucleotides. Of the four potential triphosphate-binding residues, Ser180 and Arg183 contribute significantly to k_{pol} while the effects of R149A are relatively small and are primarily on K_d, and Ser188 appears to play a minimal role in the catalysis by Pol β. These results identify several residues important for catalysis and quantitate the contributions of each of those residues. The functional data are discussed in relation to the prediction on the basis of available crystal structures.

Mammalian DNA polymerase β (Pol β)[1] has quickly become one of the best studied DNA polymerases since the gene for the enzyme was cloned in 1986 (*1*). The availability of multiple crystal structures of human and rat Pol β, including those of the enzyme complexed with both of its substrates and the metal cofactor (*2*−*4*), has aided investigations of the structure−function relationships in this enzyme (*5*−*8*). As the smallest DNA polymerase to be extensively characterized, Pol β serves as an excellent and simple model for the more complex polymerases. Although Pol β shares no significant sequence homology with the type A or B polymerase families and is instead classified as a member of a terminal transferase family of enzymes (type X) (*9*), it has a considerable number of similarities to other DNA polymerases in its structural organization. Like most other DNA polymerases, Pol β exhibits a characteristic U-shaped conformation, with three subdomains referred to as "fingers", "palm" and "thumb". [It should be noted that we have switched from our previous usage of the nomenclature of Pelletier et al. (*9*) to that of Steitz et al. (*10*) for the description of the three subdomains. We do this for more suitable comparison of functionally similar structural elements between the different polymerase families, and it involves merely reversing the labels "fingers" and "thumb".] Pol β has two intrinsic activities: nucleotidyl transferase, localized within a larger (31 kDa) domain, and deoxyribose phosphate lyase, associated with a smaller (8 kDa) N-terminal domain (*11*) which can be cleaved off by limited proteolysis (*12*).

Pol β was shown in vivo and in vitro to be an important factor in base excision repair (*13*−*15*). It serves to fill single-stranded DNA gaps, created during the repair of DNA damage caused by a variety of detrimental conditions such as UV irradiation or cytosine deamination. In general, Pol β has a lower processivity in comparison to the mammalian replicative polymerases (*16*−*18*). It is also not particularly faithful, making more misincorporations during DNA synthesis than T7 DNA polymerase or the Klenow fragment of DNA Pol I (*19*, *20*).

Using rapid chemical quench techniques and stopped-flow fluorescence, we have presented a kinetic scheme of Pol β that involves multiple conformational changes (*21*, *22*). Complete understanding of the catalytic mechanism and

[†] This work was supported by NIH Grant GM43268. The DMX-600 NMR spectrometer used was funded in part by NIH Grant RR08299 and NSF Grant BIR-9221639. This is paper 7 in the series DNA Polymerase β. For paper 6, see Ahn et al. (*18*).

* To whom correspondence should be addressed at the Department of Chemistry. Phone: (614) 292-3080. Fax: (614) 292-1532. E-mail: tsai.7@osu.edu.

[‡] Department of Biochemistry.

[§] Department of Chemistry.

[||] Also a member of the Biophysics Program and The Ohio State Biochemistry Program.

[1] Abbreviations: Pol β, rat DNA polymerase β; WT, wild type; RT, reverse transcriptase; Pol I, *Escherichia coli* DNA polymerase I; NMR, nuclear magnetic resonance; dNTP, 2′-deoxynucleoside 5′-triphosphate; NOESY, nuclear Overhauser enhanced spectroscopy.

10.1021/bi0008480 CCC: $19.00
Published on Web 11/23/2000

fidelity, however, will not be possible without quantitative evaluation, using site-specific mutagenesis, of the specific contributions of each active site residue as well as of the residues involved in conformational changes. Thus far, such studies of Pol β have been concentrated mainly on the residues in immediate contact with the base of the incoming dNTP or the complementary template DNA base (*5*−*7*). It has been demonstrated that Arg283 plays a significant role in catalytic efficiency and fidelity of DNA synthesis by Pol β, presumably through a hydrogen-bonding interaction with the templating base (*5*, *6*, *20*, *23*). In contrast, residues in contact with the base of the incoming dNTP (Tyr271 and Asn279) were shown to be less critical for both catalytic efficiency and fidelity (*6*, *7*).

In this work, we examined the catalytic functions of two groups of residues whose importance is less obvious: three residues potentially involved in the positioning or stabilization of the template DNA (Lys280, Asn294, and Glu295) and four residues hypothesized to be involved in the presumably nonspecific interactions between the polymerase and the triphosphate moiety of the incoming nucleotide (Arg149, Ser180, Arg183, and Ser188). The results provide insight into the specific functional roles of these residues and enhance our understanding of the structure−function relationships in Pol β.

MATERIALS AND METHODS

Materials. Ultrapure dNTPs, nuclease and protease activity free BSA, and G-25 microspin columns were obtained from Pharmacia Biotech. [γ-^{32}P]ATP was from ICN Pharmaceuticals, Inc. Thermostable *Pfu* DNA polymerase was from Stratagene. T4 polynucleotide kinase and *Dpn*I exonuclease were purchased from New England Biolabs. All other reagents were of the highest purity available commercially.

Mutagenesis and Enzyme Preparation. All rat DNA polymerase β mutants were created by the "QuikChange" (Stratagene) method of site-directed mutagenesis using appropriate mutagenic oligonucleotides (IDT Inc.) and wild-type Pol β plasmid [pET17b-(Pol β)] as a template according to the protocol from Stratagene. The presence of the mutations introduced and the integrity of the rest of the gene were confirmed using the ABI PRISM sequencing kit with a 373A DNA sequencer (Applied Biosystems). Pol β mutants were purified as described (*24*) (except that the affinity column was skipped) from an overexpressing *Escherichia coli* system, BL21(DE3)[plysS, pET17b-pol β] (*20*). The purity of all enzymes was assessed by SDS−PAGE analysis with silver staining (*25*). The concentrations of the enzyme solutions were determined by UV absorption, using an extinction coefficient of 21 200 $M^{-1}\cdot cm^{-1}$ at 280 nm (*26*).

Assessment of Structural Integrity of Mutant Enzymes by NMR. For the purposes of NMR analysis, Pol β samples were purified by a modified purification procedure as described (*20*). All NMR experiments were performed on a Bruker DMX-600 spectrometer. Chemical shifts were referenced to sodium [2,2,3,3-$^2H_4$]-3-(trimethylsilyl)propionate. The NMR spectra were recorded at 25 °C. Standard pulse sequence and phase cycling were used for the NOESY experiments (*27*), with a mixing time of 100 ms. All spectra were obtained in the phase-sensitive mode using time-proportional phase incrementation with water suppression using a 3-9-19 pulse sequence with gradients (*28*). The sweep widths were 13 ppm. A total of 2048 × 416 matrixes in the time domain were recorded and zero-filled to 2048 × 1024 matrixes prior to multiplication by a Gaussian function (LB2 = −3, GB2 = 0.05) in the F_2 dimension and shifted sine bell (SSB = 8) in the F_1 dimension and Fourier transformation.

DNA Substrates. Custom synthesized DNA oligomers were purchased from IDT Inc. (Coralville, IA). The DNA oligomers were further purified by electrophoresis on denaturing (7 M urea) polyacrylamide gels. Four single-nucleotide gapped DNA substrates [annealed complementary (45mer template)/(25mer primer)/(19mer downstream oligo) heteropolymeric duplexes] were used in the experiments. Sequences of the substrates used can be found in Ahn et al. (*18*). The downstream primer (19mer) was 5′-phosphorylated, and the substrates were prepared as described (*18*).

The DNA substrates were 5′-end-labeled with ^{32}P by incubation with T4 polynucleotide kinase and [γ-^{32}P]ATP (>4000 Ci/mmol) following the manufacturer's protocol. The 5′-radiolabeled DNA was separated from unreacted [γ-^{32}P]-ATP with a G-25 microspin column. The labeled DNA was mixed with ca. 100-fold molar excess of unlabeled, the solution was heated to 85 °C for 5 min, and the solution was then slowly cooled to room temperature.

Pre-Steady-State Kinetic Experiments and Product Analyses. An RQF-3 rapid chemical quench instrument (KinTek Instrument Corp., State College, PA) was used for reaction times ranging from 5 ms to 20 s. Pol β was preincubated with the DNA substrate prior to rapid mixing with dNTP and $MgCl_2$ to begin the reaction, which was quenched with 0.6 M Na_4EDTA (pH 8.0). For reaction times greater than 20 s, 15 μL aliquots of the reaction mixture (total volume 150 μL) were removed and mixed with equal volumes of quench solution after the desired time interval. The typical experiment was performed at 37 °C in 50 mM Tris·HCl, pH 7.7, containing 50 mM KCl, 10% glycerol, 100 μg/mL BSA, 1 mM DTT, 2.5 mM $MgCl_2$ (free), and varying [dNTP]. A 5-fold excess concentration of the enzyme (500 nM in the reaction mixture) relative to the DNA duplex substrate (100 nM) was used for all assays. Under these conditions, >90% of the DNA substrate should be complexed to the enzyme (*20*), and the reaction time course is represented as a single turnover burst phase of dNTP incorporation, with a negligible linear phase due to a low number of enzyme dissociation/rebinding events (*18*).

A sample of the quenched reaction (20 μL) was mixed with an equal volume of gel loading buffer (*29*), denatured at 85 °C for 5 min, and run on 16% polyacrylamide (19:1 acrylamide:bisacrylamide)−7 M urea gel (50 cm × 38 cm × 0.4 mm). The disappearance of substrate (25mer) and the formation of product (26mer) were quantified with a STORM 840 PhosphorImager (Molecular Dynamics).

Data Analysis. Most of the data were fitted by nonlinear regression using Sigma Plot software (Jandel Scientific) with the appropriate equations as described earlier (*18*). Time curves for the formation of the product DNA (26mer) were fitted with eq 1 to determine the apparent burst rate constant (k_{obs}) for each particular concentration of dNTP:

$$[26mer] = A[1 - \exp(-k_{obs}t)] \quad (1)$$

where A represents the burst amplitude. The apparent

catalytic rates, $k_{app,}$ were plotted against dNTP concentrations, and the data were fitted with the hyperbolic eq 2 to determine k_{pol} and the apparent dissociation constant for dNTP (K_d):

$$k_{app} = (k_{pol}[\text{dNTP}])/([\text{dNTP}] + K_d) \quad (2)$$

Fidelity (F) of DNA synthesis was calculated using the equation:

$$F = [(k_{pol}/K_d)_c + (k_{pol}/K_d)_i]/(k_{pol}/K_d)_i \quad (3)$$

where c and i represent correct and incorrect incorporations, respectively.

Measurement of DNA Binding Affinity. The DNA binding affinity for WT Pol β and some of the potentially important template-positioning mutants was tested using a gel mobility shift assay. Radiolabeled DNA substrate for this assay was prepared as described above. For a typical gel shift assay, varying concentrations of protein were added to the binding mixture containing ca. 1 nM DNA substrate in 50 mM Tris·HCl, pH 8.0, 50 mM KCl, 5 mM $MgCl_2$, and 10% (v/v) glycerol. The reaction samples were then incubated at 25 °C for 10 min and loaded onto an 8% polyacrylamide gel (8.0 cm × 7.3 cm × 0.5 mm) that had been prerun for 1 h at 4 °C in TBE buffer (90 mM Tris·borate, 2 mM Na_2EDTA, pH 8.3). After being run about 4 h at 58 V at 4 °C, the gel was exposed to a phosphor screen and quantified with the STORM 840 PhosphorImager.

RESULTS

Rationale of Our Approaches. Although our experimental approaches are similar to those used in our previous publications (*5*, *18*, *20*), it is important to reiterate the significance of our approaches in relation to the vast amount of structural information and other biochemical studies related to Pol β. The residues in this work were chosen because they either appear to be or have been explicitly suggested to be important on the basis of crystal structures. However, crystal structures represent static complexes of ground states (free enzyme, E·DNA binary complex, or E·DNA·MgdNTP ternary complex) in the catalytic pathway. Our goal is to understand the mechanism of catalysis in kinetic and energetic terms, which is not provided by crystal structures. Furthermore, the use of pre-steady-state kinetics in this work provides a more in-depth evaluation of kinetic properties.

Identification of Template-Positioning Residues from Crystal Structures. On the basis of the crystal structures of Pol β complexed with DNA and nucleotide (*3*, *30*), four active site residues (Lys280, Arg283, Asn294, and Glu295) are located proximal to the template DNA strand such that potentially important interactions between these residues and the template appear likely. As shown in Figure 1A−C, Arg283, Asn294, and Glu295 move into close contact with the template strand in the ternary complex. It appears that the side chains of Glu295 and Asn294 are positioned for steric contact and possibly hydrogen bonding (Asn294) with the deoxyribose phosphate backbone of the template (Figure 1B). X-ray crystallographic studies have shown that the region of the template strand which shifts position upon nucleotide binding (Figure 1C) also experiences a significant decrease in *B*-factor—67 to 48 on average for residues G6 to C8, for example—suggesting that this region of the template strand becomes more ordered in the ternary

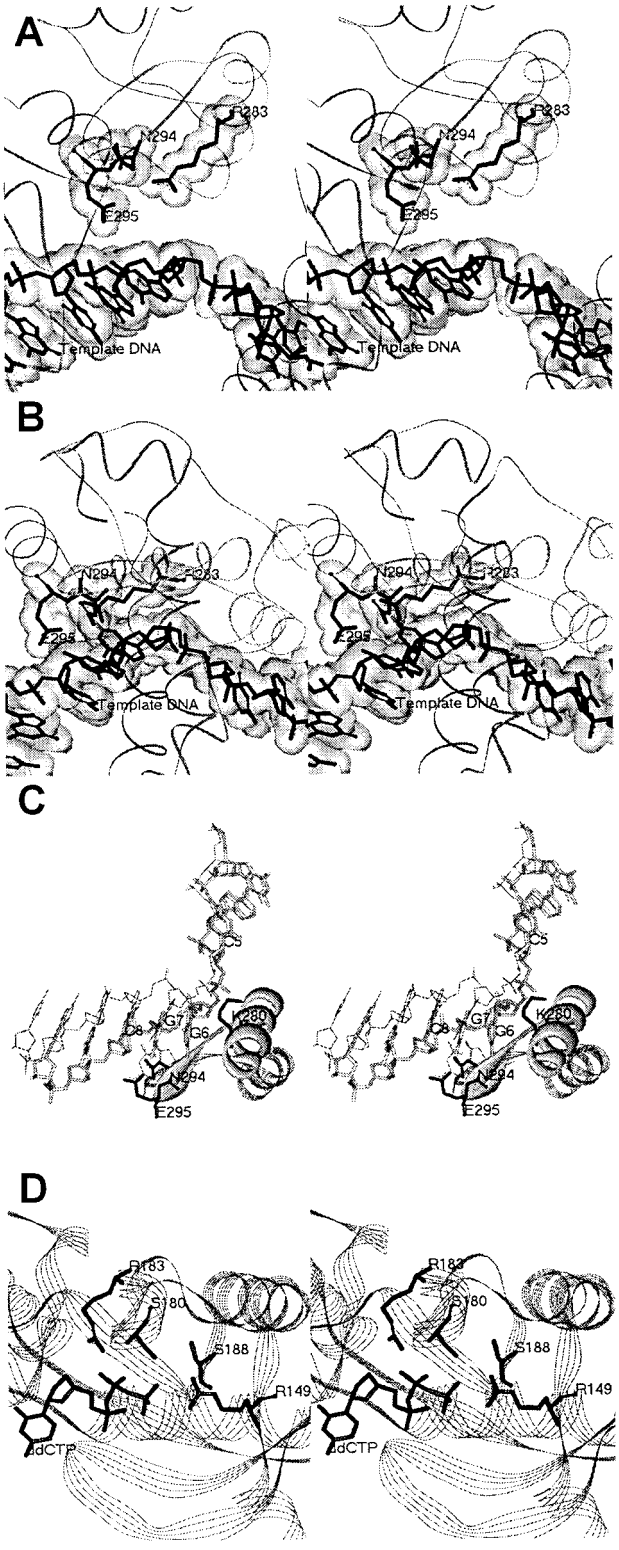

FIGURE 1: Stereoviews of the residues studied and their local environments. R283, N294, and E295 with template DNA in the binary (A) and ternary complex (B). Superposition of the binary and ternary complexes showing the local environment around the template strand and including N294, E295, and K280 (C). In (C), thick lines show the ternary complex and thin lines indicate the binary complex. All labels in (C) are for the ternary complex. Local environment around the incoming nucleoside triphosphate in the ternary complex (D). Each figure was adapted from PDB file 1BPX and/or 1BPY (*3*).

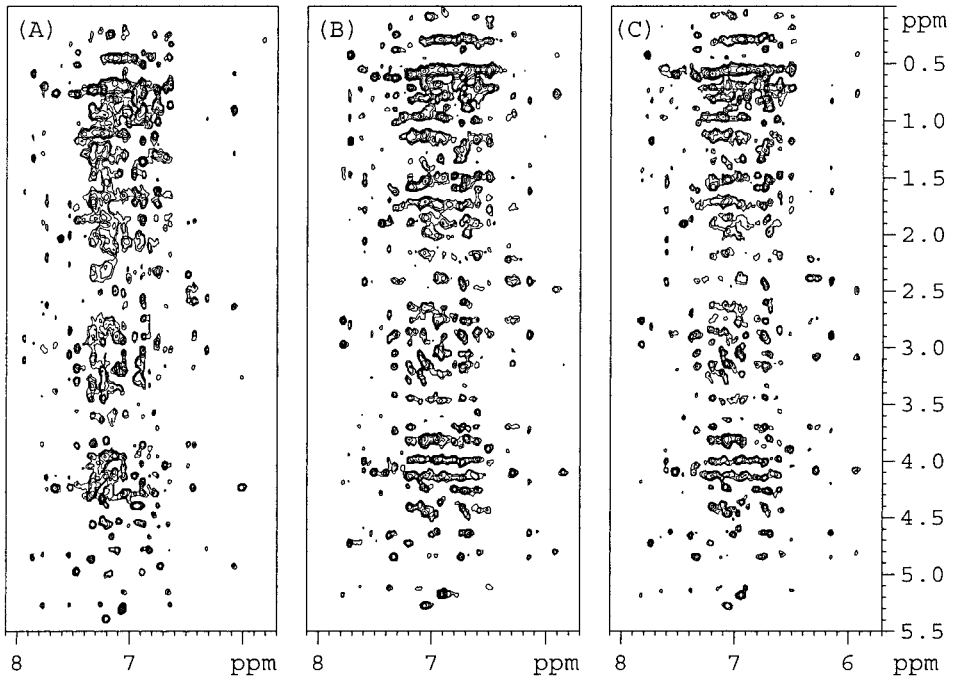

FIGURE 2: 2D NOESY proton NMR spectra wild-type Pol β (A), S180A (B), and E295A (C). The NMR samples contained 0.3 mM enzyme in D_2O at pH 7.5. The spectra were recorded at 25 °C with a mixing time of 100 ms.

complex. The overall *B*-factors for the template strands in the two structures are essentially the same (57 vs 52). Lys280 is also in a position to have potentially important ineractions with the template, in this case providing steric constraint on the templating base (G6) opposite the incoming dNTP (Figure 1C). Such an interaction has been proposed to be of importance to the incorporation fidelity of polymerases (*31*, *32*).

Since Arg283 appears to be hydrogen bonded to the template base opposite the incoming dNTP (*30*), it has been the focus of previous studies. It was found that substitution of Arg283 leads to a significant loss of fidelity of DNA synthesis and catalytic efficiency by the enzyme (*5*, *6*). Thus this paper focuses on the roles of the other three residues.

Possible Triphosphate-Binding Residues from Crystal Structures. Four residues, Arg149, Ser180, Arg183, and Ser188, can be considered as possible residues interacting with the triphosphate moiety of the incoming dNTP on the basis of crystal structures. In the ternary complex with dNTP and *gapped* substrate (Figure 1D), Arg183 appears to interact with the β-phosphate, and Ser180 is positioned to interact with both the β- and γ-phosphates. These two residues are expected to play significant catalytic roles. The other two residues, Arg149 and Ser188, appear to be less certain. They could potentially interact with the γ-phosphate, but the distances are slightly beyond the range that would predict a hydrogen-bonding interaction. Since the distances are smaller in a different form of the crystal structure, that with *nongapped* template/primer (*30*), these two residues could potentially be involved in catalysis. In this study we test the functional roles of all four residues by use of gapped substrates.

Construction and Purification of Mutants. To test the specific functional roles of the candidate residues mentioned above, we created alanine mutants at each of these positions. In addition, a conservative Gln mutant was also created for Asn294. All mutant enzymes were purified according to the procedure developed for the wild-type Pol β as has been previously described (*20*). Mutant proteins behaved similarly to wild type during purification, and comparable yields were generally obtained.

Mutations Introduced Have Little Effect on the Structural Properties of Pol β. The effects on the overall structure of Pol β attributable to the mutations introduced were evaluated by means of 1D ^{1}H NMR and 2D NOESY NMR. Representative 2D NOESY spectra (wild-type Pol β and S180A and E295A mutants) are shown in Figure 2. As can be seen from the figure, the mutant spectra appear to be similar to that of the wild-type Pol β spectrum. The other mutants exhibited similar spectra as well. On the basis of the NMR analyses, we concluded that the functional changes observed in the mutant enzymes are not likely to be caused by significant alterations in the global conformation of the enzyme but rather by the missing functionality of the particular residue.

Pre-Steady-State Kinetic Analysis of Mutants. Single-nucleotide gapped DNA was used in this study. This type of DNA has been shown previously to be the substrate preferred by Pol β in vitro, presumably due to better mimicking of the natural substrate utilized by the enzyme during base excision repair (*14*, *16*). The k_{pol}, K_d, k_{pol}/K_d, and fidelity values were determined as described in Materials and Methods. A representative plot is shown in Figure 3. All mutants were characterized with multiple base pair combinations including both correct and incorrect base pairs. A recently completed kinetic analysis of wild-type Pol β with all 16 possible base pairs (*18*) was used as a reference by which to judge kinetic perturbation in the mutant enzymes. The calculated kinetic constants along with comparisons to WT are shown in Table 1.

In Table 1, changes (increases or decreases relative to the WT data) of kinetic parameters are indicated in parentheses,

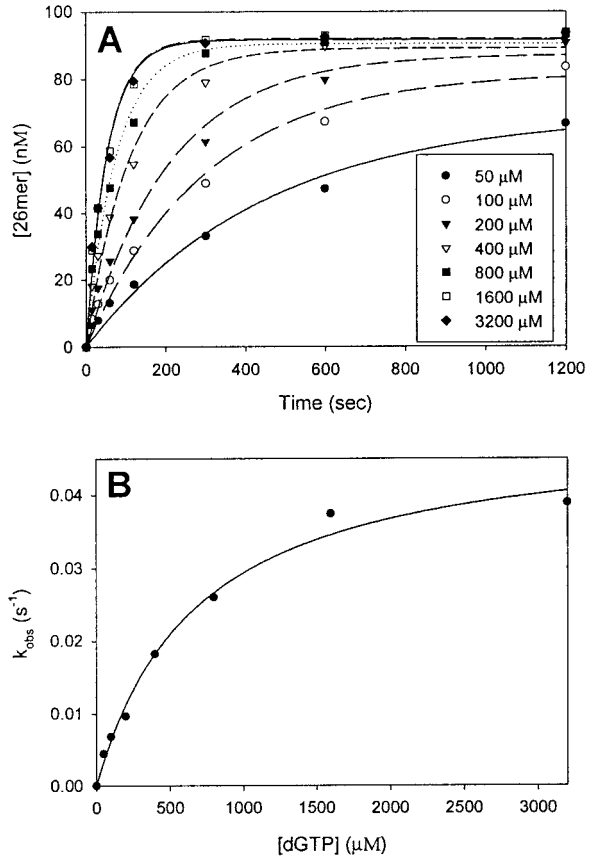

FIGURE 3: Pre-steady-state kinetics of dGTP incorporation opposite template T catalyzed by mutant Pol β N294Q. The reaction conditions and methods of product analysis were as described in the Materials and Methods section. (A) Product vs time plot. DNA substrate (100 nM) was preincubated with 500 nM Pol β and then mixed with 50, 100, 200, 400, 800, 1600, or 3200 μM dGTP. The reaction was quenched with 0.6 M Na_2EDTA after 15, 30, 60, 120, 300, 600, and 1200 s. The results were fit to a single-exponential equation (eq 1) to obtain k_{obs} for each dGTP concentration. (B) dGTP concentration dependence curve. k_{pol} and K_d were determined to be 0.049 ± 0.002 s^{-1} and 670 ± 96 μM, respectively, by fitting to the hyperbolic equation (eq 2).

and only those greater than 5-fold are further interpreted. The results indicate several significant perturbations in the kinetic parameters of the mutant enzymes. Of the four mutants of the three possible template-positioning residues, K280A is altered only slightly relative to WT while the other three mutants, N294A, N294Q, and E295A, display reduced pre-steady-state catalytic rates (up to 870-fold decrease in k_{pol}). In each case, the perturbation for incorrect base pairs was greater than that for correct base pairs. This difference in perturbation for correct vs incorrect base pairs was greatest for N294Q, which resulted in improved overall fidelity for N294Q by up to 19-fold. E295A also appears to have elevated K_d's for correct nucleotides. The other three mutants show apparently unchanged K_d's for both correct and incorrect nucleotides.

Two of the four mutants of the putative dNTP triphosphate-binding residues (R183A and S180A) also display substantial decreases in k_{pol} for both correct and incorrect base pairs. Additionally, R149A and S180A appear to exhibit an increased K_d for correct nucleotides but generally not for incorrect ones in the case of R149A.

Comparison of DNA Binding Affinity between WT Pol β and Mutants. To test whether DNA binding is perturbed in the mutants E295A, N294A, and N294Q, a gel mobility shift assay was performed for WT Pol β and these three mutants. As shown in Figure 4, two major bound species can be seen in the gel. We interpret the faster running of the shifted bands

Table 1: Kinetic Parameters for Wild-Type and Mutant Pol β Enzymes

enzyme	base pair[a]	k_{pol}, s^{-1}	K_d, μM	k_{pol}/K_d, $s^{-1}\,M^{-1}$	fidelity[b]
wild type[c]	A·T	21.9	5.4	4 100 000	
	T·A	36.3	8.5	4 300 000	
	G·C	12.5	1.9	6 600 000	
	C·G	18.4	3.6	5 100 000	
	A·A	0.031	310	100	41 000
	A·C	0.23	190	1 200	3 400
	T·G	0.96	620	1 500	2 800
	T·C	1.3	510	2 500	1 700
	G·A	0.019	270	70	93 000
	G·T	0.37	650	570	12 000
	C·A	0.24	470	510	10 000
	C·T	0.22	877	250	20 000
		DNA template-positioning residues			
N294A	A·T	0.53 (41↓)	14 (2.6↑)	38 000 (108↓)	
	T·A	0.49 (74↓)	21.5 (2.5↑)	23 000 (190↓)	
	G·C	4.0 (3.1↓)	6.6 (3.5↑)	600 000 (11↓)	
	A·A	0.000 65 (48↓)	110 (2.8↓)	5.9 (16.9↓)	6 500 (6.3↓)
	T·G	0.004 (240↓)	540 (1.1↓)	7.4 (200↓)	3 100 (1.1↑)
	T·C	0.009 2 (141↓)	1 160 (2.3↑)	7.9 (320↓)	2 900 (1.7↑)
	G·A	0.000 56 (34↓)	230 (1.2↓)	2.5 (28↓)	240 000 (2.6↑)
N294Q	A·T	3.5 (6.3↓)	13 (2.4↑)	260 000 (15.8↓)	
	T·A	4.2 (8.6↓)	15 (1.8↑)	280 000 (15.4↓)	
	G·C	2.6 (4.8↓)	1.6 (1.2↓)	1 625 000 (4.1↓)	
	A·A	0.000 8 (39↓)	420 (1.4↑)	1.9 (52.6↓)	137 000 (3.3↑)
	T·G	0.049 (20↓)	670 (2.5↓)	73 (16.1↓)	3 800 (1.4↑)
	T·C	0.005 (260↓)	585 (1.1↑)	8.5 (294↓)	33 000 (19.4↑)
	G·T	0.005 3 (70↓)	750 (1.2↑)	7.1 (80.3↓)	230 000 (19.2↑)
	G·A	0.000 65 (29↓)	180 (1.5↓)	3.6 (19.4↓)	450 000 (4.8↑)
E295A	A·T	0.43 (51↓)	106 (19.6↑)	4 060 (1010↓)	
	T·A	0.14 (260↓)	42 (4.9↑)	3 300 (1300↓)	
	G·C	2.0 (6.3↓)	10 (5.3↑)	200 000 (33↓)	
	A·A	0.000 3 (103↓)	260 (1.2↓)	1.3 (76.9↓)	3 100 (13.2↓)
	T·G	0.001 1 (872↓)	850 (1.4↑)	1.3 (1150↓)	2 600 (1.1↓)
	T·C	0.006 3 (206↓)	890 (1.7↑)	7.1 (352↓)	470 (3.6↓)
	G·A	0.000 23 (85↓)	295 (1.1↑)	0.78 (89.7↓)	250 000 (2.7↑)
K280A	T·A	20 (1.8↓)	11 (1.3↑)	1 800 000 (2.4↓)	
	G·C	12 (1.0↓)	6 (3.2↑)	2 000 000 (3.3↓)	
	T·G	0.77 (1.2↓)	1 050 (1.7↑)	730 (2.1↓)	2 300 (1.2↓)
	T·C	1.3 (1.0)	520 (1.0↑)	2 500 (1.0↓)	720 (2.4↓)
	G·A	0.012 (1.6↓)	495 (1.8↑)	24 (2.9↓)	83 000 (1.1↓)
	G·T	0.21 (1.8↓)	970 (1.5↑)	220 (2.6↓)	9 100 (1.3↓)
		dNTP triphosphate-binding residues			
S180A	A·T	1.0 (21.9↓)	70 (13.0↑)	14 300 (287↓)	
	T·A	0.57 (63.7↓)	59 (7.0↑)	9 800 (439↓)	
	A·A	0.000 095 (326↓)	300 (1.0↑)	0.32 (313↓)	45 000 (1.1↑)
	A·C	0.003 5 (66↓)	2 050 (10.8↑)	1.7 (706↓)	8 400 (2.5↑)
	T·G	0.005 3 (181↓)	2 000 (3.2↑)	2.6 (577↓)	3 800 (1.4↑)
	T·C	0.004 (325↓)	1 850 (3.6↑)	2.2 (1140↓)	4 500 (2.6↑)
R183A	A·T	0.9 (24.3↓)	21 (3.9↑)	43 000 (95↓)	
	T·A	0.83 (43.7↓)	87 (10↑)	9 500 (450↓)	
	G·C	2.6 (4.8↓)	5.9 (3.1↑)	440 000 (15↓)	
	A·C	0.009 (26↓)	615 (3.2↑)	14.6 (82↓)	2 950 (1.2↓)
	T·G	0.016 (60↓)	670 (1.1↑)	24 (63↓)	400 (7.0↓)
	T·C	0.013 (100↓)	520 (1.0↑)	25 (100↓)	380 (4.5↓)
	G·A	0.000 25 (76↓)	145 (1.9↓)	1.7 (41.2↓)	260 000 (2.8↑)
	G·T	0.003 2 (116↓)	1 250 (1.9↑)	2.6 (219↓)	170 000 (14↑)
R149A	A·T	24 (1.1↑)	35 (6.5↑)	685 000 (6.0↓)	
	T·A	21 (1.7↓)	109 (12.8↑)	193 000 (22.3↓)	
	G·C	11 (1.1↓)	12 (6.3↑)	920 000 (7.2↓)	
	A·C	0.5 (2.2↑)	1 600 (1.3↑)	312 (3.8↓)	2 200 (1.5↓)
	T·G	0.38 (2.5↓)	470 (3.2↓)	800 (1.9↓)	240 (11.7↓)
	G·A	0.025 (1.3↑)	1 500 (5.6↑)	17 (4.1↓)	54 000 (1.7↓)
S188A	A·T	8.9 (2.5↓)	3.8 (1.4↓)	2 400 000 (1.7↓)	
	C·G	6.1 (2.0↓)	7.9 (4.2↑)	780 000 (8.5↓)	
	A·A	0.027 (1.1↓)	1 050 (3.4↑)	26 (3.8↓)	92 000 (2.2↑)
	A·C	0.35 (1.5↑)	1 700 (8.9↑)	208 (5.8↓)	11 500 (3.4↑)
	C·A	0.1 (2.4↓)	750 (1.6↑)	133 (3.8↓)	5 900 (1.7↓)
	C·T	0.17 (1.3↓)	2 100 (2.4↑)	80 (3.1↓)	9 600 (2.1↓)

[a] In the base pair notation X·Y, X is the templating base and Y is the incoming nucleotide. [b] Fidelity $= [(k_{pol}/K_d)_c + (k_{pol}/K_d)_i]/(k_{pol}/K_d)_i$. [c] Taken from Ahn et al. (*18*).

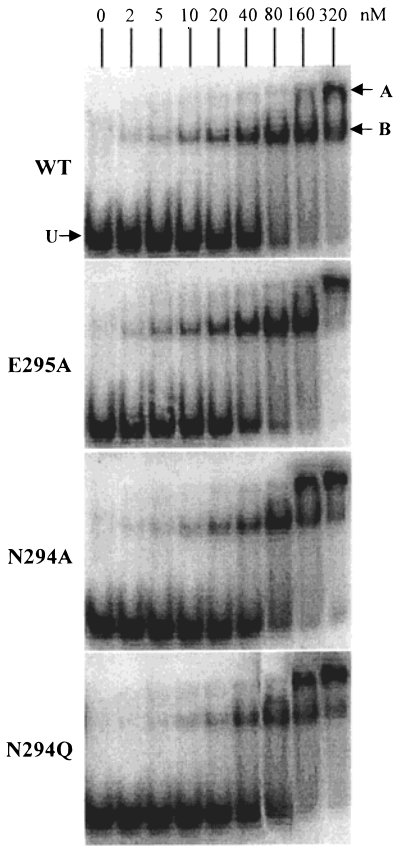

FIGURE 4: Comparison of DNA binding affinity of WT Pol β and mutants using a gel mobility shift assay. Different concentrations of WT Pol β and mutants were incubated with 5′-labeled DNA substrate (1 nM) for 10 min at 25 °C, and the mixture was then loaded onto an 8% native polyacrylamide gel and run at 4 °C as described.

as being the 1:1 enzyme−DNA complex (B in Figure 4), while the more slowly migrating complex (A in Figure 4), which appears at higher protein concentrations, likely contains one or more additional protein molecules per DNA substrate. The results demonstrate that E295A, N294A, and N294Q Pol β mutants have approximately similar DNA binding affinity as WT, suggesting that the corresponding residues have little effect on DNA binding in the ground state. This is consistent with the crystallographic evidence which shows no interaction between these residues and the DNA, as illustrated in Figure 1A,C.

The interpretation of kinetic and DNA binding data in reference to the potential functional roles of the specific residues is elaborated in the Discussion.

DISCUSSION

Template-Positioning Residues Asn294 and Glu295, Not Lys280, Contribute Significantly to Catalytic Efficiency. Of the three residues selected and examined on the basis of crystal structures, Asn294 and Glu295 appear to contribute significantly to the catalytic function of Pol β, as suggested by the large decreases in the k_{pol} values of N294A, N294Q, and E295A. Without considering the structural information, the results would suggest that Asn294 and Glu295 stabilize the transition state. On the basis of the structural information, one can say that these two residues stabilize the transition state by helping to position the template DNA properly. As shown in Figure 1A−C, such positioning occurs only in the ternary complex, not the binary complex. This point is supported by the observation that these mutants showed unchanged ground-state DNA binding affinity, as indicated by the band-shift assays in Figure 4. Central to any discussion of k_{pol} effects is a knowledge of the rate-limiting step in the kinetic mechanism. While a conformational change step has been proposed to be rate-limiting for several DNA polymerases (*33*, *34*), including Pol β (*20*), recent results from our laboratory (unpublished data) bring this conclusion into doubt, at least in the case of this enzyme. Therefore, we interpret changes in k_{pol} to reflect altered ability of the mutant to stabilize the transition state of phorphoryl transfer.

On the basis of the crystal structures, the conformational difference between the binary and the ternary complexes involves closing of the fingers subdomain. Our results, in combination with the existing structural data, suggest that these residues have a direct interaction with substrate after the closing of the fingers subdomain and that this interaction serves to maintain the DNA template in a position ready for catalysis. Without this positioning effect, catalysis is severely hindered.

The observation that the K_d(dNTP) values (dissociation constants of dNTP) of these mutants have not been perturbed relative to WT (with the exception of E295A with correct base pairs; see later section) is in agreement with the information from the crystal structures that these two residues are *not* in direct contact with the incoming dNTP. Taken together, our results suggest that, even though Asn294 and Glu295 do not interact directly with the incoming dNTP (like residues Tyr271 and Asn279 described in Beard et al. and Kraynov et al.) or the template base opposite the incoming dNTP (like Arg283 described in Ahn et al. etc.), they can stabilize the transition state during catalysis by interacting with the backbone of the DNA template.

Possible Roles of Lys280. On the other hand, the activity of the K280A mutant was essentially unperturbed relative to WT. Lys280 is located in a 90° kink of the template DNA strand in a position apparently suited for stacking against the template base that is opposite the incoming dNTP (Figure 1C). On the basis of the structural data of Pol β in a ternary complex with dNTP and gapped substrate (*3*), this residue appears to be close enough to this template base to restrain its movement via steric contact. It has been suggested (*31*, *32*) that such interactions may create an important steric constraint on the nascent base pair. Such a constraint should favor geometrically compact Watson−Crick base pairs relative to incorrect base pairs and thus may constitute one mechanism for discrimination. Our results indicate that the bulk of the Lys280 side chain confers no significant advantage in either catalytic efficiency or fidelity by the enzyme. This may imply several possibilities. It could be argued that the β-carbon of Lys280 (or the helix backbone) provides the necessary steric stabilization of the template base and that the remainder of the residue is superfluous. However, as shown in Figure 1C, the structural data might lead one to believe that the full lysine side chain would provide additional stabilization. Alternatively, closer contact than is provided by Lys280 may be required in order to have an effect on fidelity or catalysis. A third possibility is that steric restraint applied directly to the template base is not a particularly important fidelity enhancing mechanism.

Improved Fidelity for N294Q. Interestingly, the catalytic rate is partially restored upon changing residue 294 from Ala to Gln, but only for correct base pairs. This suggests that the N294Q mutant is capable of providing the necessary contact with template to maintain and stabilize its position at the transition state. Nonetheless, incorrect base pair formation is catalyzed no better by N294Q than by N294A. This resulted in an improved fidelity (up to 19-fold) for some of the base pairs. An improvement in fidelity of this magnitude is very uncommon for DNA polymerases, even though it is only for particular base pairs. The observation that the N294Q mutant has enhanced fidelity relative to WT suggests that transition state stabilization via steric interaction between the protein and the template backbone may be an important fidelity-enhancing mechanism. To our knowledge, this is the first demonstration of an increased fidelity for a polymerase mutant in which the mutated position was involved in direct contact with the template backbone.

Additional Role for Glu295. The E295A mutant appeared to be generally perturbed to a slightly greater degree than did N294A. This may reflect a possible dual role of this residue. In the inactive binary complex, Pol β appears to have one of its essential Asp residues "tied up" in a salt bridge with Arg258. It has been shown that, upon closure of the fingers subdomain during a conformational transition from the inactive to the active form of the enzyme, Glu295 may form a salt bridge with Arg258, helping to free Asp192 for coordinating the catalytic Mg^{2+} ion (*4*). In the case of E295A, the binding partner of Arg258 would be eliminated. This may trigger Asp192 to remain hydrogen-bonded to Arg258 and the enzyme to exist in an inactive conformation, as manifested in a lower catalytic efficiency. As Asp192 is also involved in coordinating the nucleotide binding Mg^{2+}, this may also explain why E295A is the only one of these three mutants to display significant elevations in the dissociation constant of MgdNTP, K_d(dNTP), for correct base pairs (see Table 1: 5-fold for T·A and G·C; 20-fold for A·T).

Contributions of Triphosphate-Binding Residues to Catalytic Efficiency. In contrast to the template-positioning residues, the triphosphate-binding residues are likely to be involved in directly stabilizing the transition state of the reaction. It seems likely that interactions with the β-phosphate would be important to orient this leaving group for the forthcoming S_N2 attack by the primer's 3′-hydroxyl and possibly to position the α-phosphate in an orientation optimal for this attack. Interactions with γ-phosphate, on the other hand, are less likely to play a direct role in chemistry but rather would likely serve the purpose of increasing the binding affinity for incoming nucleotide.

Ser180 and Arg183. As explained earlier and illustrated in Figure 1D, in the crystal structures of ground-state complexes Arg183 interacts with the β-phosphate in both the nongapped ternary complex and the gapped ternary complex, but the role of Ser180 is uncertain. The results in Table 1 show that both S180A and R183A display significant decreases (up to 326-fold) in k_{pol} for both correct and incorrect base pairs. They also showed sporadic and modest increases in K_d (up to 13-fold). In both cases the increases in K_d seem to be more applicable to correct base pairs. The fidelity is largely unchanged for both mutants. These results suggest that Ser180 and Arg183 are important for stabilizing the transition state during catalysis, possibly by orienting the leaving group (β-phosphate) at the transition state.

Arg149 and Ser188. These two residues are suspected, on the basis of crystal structures, to interact with the γ-phosphate of the incoming dNTP. As shown in Table 1, the changes in kinetic parameters are very small for both R149A and S188A mutants. In the case of R149A, the only effect was a modest increase in K_d(dNTP) for correct base pairs (by 6−13-fold). This suggests that Arg149 does interact with dNTP but that this interaction only confers a stabilization in the ground-state complex. The S188A mutant had no significant perturbations other than a 9-fold increase in K_d for the A·C mispair. This result suggests that Ser188 plays a minimal role in catalysis by Pol β.

Conclusion. On the basis of crystal structures, we have identified several potential template-positioning residues and dNTP triphosphate-binding residues. Specific contributions of these residues to the catalytic function have been tested by site-directed mutagenesis and pre-steady-state kinetic analysis. The results suggest that two of the three template-positioning residues (Asn294 and Glu295) contribute significantly to k_{pol} possibly by helping to stabilize the transition state via positioning the DNA template. A notable improvement in fidelity was also observed for N294Q. On the other hand, the K280A mutant surprisingly behaves similarly to WT Pol β. Of the four potential triphosphate-binding residues, our results suggest that Ser180 and Arg183 are important for transition state stabilization possibly by interacting primarily with the β-phosphate, that Arg149 is likely to contribute to dNTP binding by interacting with the γ-phosphate, and that Ser188 plays a minimal role in catalysis by Pol β. Overall, our results provide quantitative contributions by the two types of residues whose catalytic roles were not obvious. The functional results, along with the previous structural information, allowed us to further pinpoint the functional roles of specific residues.

ACKNOWLEDGMENT

The authors thank Dr. Chunhua Yuan for his assistance in preparing figures and analyzing structural data.

REFERENCES

1. Zmudzka, B. Z., SenGupta, D., Matsukage, A., Cobianchi, F., Kumar, P., and Wilson, S. H. (1986) *Proc. Natl. Acad. Sci. U.S.A. 83*, 5106−5110.
2. Sawaya, M. R., Pelletier, H., Kumar, A., Wilson, S. H., and Kraut, J. (1994) *Science 264*, 1930−1935.
3. Sawaya, M. R., Prasad, R., Wilson, S. H., Kraut, J., and Pelletier, H. (1997) *Biochemistry 36*, 11205−11215.
4. Pelletier, H., Sawaya, M. R., Wolfle, W., Wilson, S. H., and Kraut, J. (1996) *Biochemistry 35*, 12742−12761.
5. Ahn, J., Werneburg, B. G., and Tsai, M. D. (1997) *Biochemistry 36*, 1100−1107.
6. Beard, W. A., Osheroff, W. P., Prasad, R., Sawaya, M. R., Jaju, M., Wood, T. G., Kraut, J., Kunkel, T. A., and Wilson, S. H. (1996) *J. Biol. Chem. 271*, 12141−12144.
7. Kraynov, V. S., Werneburg, B. G., Zhong, X., Lee, H., Ahn, J., and Tsai, M. D. (1997) *Biochem. J. 323* (Part 1), 103−111.
8. Washington, S. L., Yoon, M. S., Chagovetz, A. M., Li, S. X., Clairmont, C. A., Preston, B. D., Eckert, K. A., and Sweasy, J. B. (1997) *Proc. Natl. Acad. Sci. U.S.A. 94*, 1321−1326.
9. Pelletier, H. (1994) *Science 266*, 2025−2026.
10. Steitz, T. A., Smerdon, S. J., Jager, J., and Joyce, C. M. (1994) *Science 266*, 2022−2025.

11. Matsumoto, Y., and Kim, K. (1995) *Science 269*, 699−702.
12. Kumar, A., Widen, S. G., Williams, K. R., Kedar, P., Karpel, R. L., and Wilson, S. H. (1990) *J. Biol. Chem. 265*, 2124−2131.
13. Singhal, R. K., Prasad, R., and Wilson, S. H. (1995) *J. Biol. Chem. 270*, 949−957.
14. Sobol, R. W., Horton, J. K., Kühn, R., Gu, H., Singhal, R. K., Prasad, R., Rajewsky, K., and Wilson, S. H. (1996) *Nature 379*, 183−186.
15. Nicholl, I. D., Nealon, K., and Kenny, M. K. (1997) *Biochemistry 36*, 7557−7566.
16. Singhal, R. K., and Wilson, S. H. (1993) *J. Biol. Chem. 268*, 15906−15911.
17. Prasad, R., Beard, W. A., and Wilson, S. H. (1994) *J. Biol. Chem. 269*, 18096−18101.
18. Ahn, J., Kraynov, V. S., Zhong, X., Werneburg, B. G., and Tsai, M. D. (1998) *Biochem. J. 331*, 79−87.
19. Kunkel, T. A., and Alexander, P. S. (1986) *J. Biol. Chem. 261*, 160−166.
20. Werneburg, B. G., Ahn, J., Zhong, X., Hondal, R. J., Kraynov, V. S., and Tsai, M. D. (1996) *Biochemistry 35*, 7041−7050.
21. Zhong, X., Patel, S. S., Werneburg, B. G., and Tsai, M. D. (1997) *Biochemistry 36*, 11891−11900.
22. Zhong, X., Patel, S. S., and Tsai, M.-D. (1998) *J. Am. Chem. Soc. 120*, 235−236.
23. Osheroff, W. P., Beard, W. A., Wilson, S. H., and Kunkel, T. A. (1999) *J. Biol. Chem. 274*, 20749−20752.
24. Date, T., Yamaguchi, M., Hirose, F., Nishimoto, Y., Tanihara, K., and Matsukage, A. (1988) *Biochemistry 27*, 2983−2990.
25. Merril, C. R., Goldman, D., and Van Keuren, M. L. (1984) *Methods Enzymol. 104*, 441−447.
26. Casas-Finet, J. R., Kumar, A., Morris, G., Wilson, S. H., and Karpel, R. L. (1991) *J. Biol. Chem. 266*, 19618−19625.
27. Bodenhausen, G., Kogler, H., and Ernst, R. R. (1984) *J. Magn. Reson. 58*, 370−388.
28. Piotto, M., Saudek, V., and Sklenár, V. (1992) *J. Biomol. NMR 2*, 661−665.
29. Maniatis, T., Fritsch, E. F., and Sambrook, J. (1982) *Molecular Cloning*: *A Laboratory Manual*, Cold Spring Harbor Laboratory Press, Cold Spring Harbor, NY.
30. Pelletier, H., Sawaya, M. R., Kumar, A., Wilson, S. H., and Kraut, J. (1994) *Science 264*, 1891−1903.
31. Doublié, S., Tabor, S., Long, A. M., Richardson, C. C., and Ellenberger, T. (1998) *Nature 391*, 251−258.
32. Kiefer, J. R., Mao, C., Braman, J. C., and Beese, L. S. (1998) *Nature 391*, 304−307.
33. Bryant, F. R., Johnson, K. A., and Benkovic, S. J. (1983) *Biochemistry 22*, 3537−3546.
34. Patel, S. S., Wong, I., and Johnson, K. A. (1991) *Biochemistry 30*, 511−525.

BI0008480